LI
LABORATORY INVESTIGATION
THE BASIC AND TRANSLATIONAL PATHOLOGY RESEARCH JOURNAL
VOLUME 99 | SUPPLEMENT 1 | MARCH 2019

USCAP 2019

ABSTRACTS

CARDIOVASCULAR PATHOLOGY (299-316)

USCAP 108TH ANNUAL MEETING

UNLOCKING YOUR INGENUITY

MARCH 16-21, 2019

National Harbor, Maryland
Gaylord National Resort & Convention Center

Published by
SPRINGER NATURE
www.ModernPathology.org

USCAP Creating a Better Pathologist
AN OFFICIAL JOURNAL OF THE UNITED STATES AND CANADIAN ACADEMY OF PATHOLOGY

EDUCATION COMMITTEE

Jason L. Hornick, Chair
Rhonda K. Yantiss, Chair, Abstract Review Board and Assignment Committee
Laura W. Lamps, Chair, CME Subcommittee
Steven D. Billings, Interactive Microscopy Subcommittee
Shree G. Sharma, Informatics Subcommittee
Raja R. Seethala, Short Course Coordinator
Ilan Weinreb, Subcommittee for Unique Live Course Offerings
David B. Kaminsky (Ex-Officio)
Aleodor (Doru) Andea
Zubair Baloch
Olca Basturk
Gregory R. Bean, Pathologist-in-Training
Daniel J. Brat
Ashley M. Cimino-Mathews
James R. Cook
Sarah M. Dry
William C. Faquin
Carol F. Farver
Yuri Fedoriw
Meera R. Hameed
Michelle S. Hirsch
Lakshmi Priya Kunju
Anna Marie Mulligan
Rish Pai
Vinita Parkash
Anil Parwani
Deepa Patil
Kwun Wah Wen, Pathologist-in-Training

ABSTRACT REVIEW BOARD

Benjamin Adam
Michelle Afkhami
Narasimhan (Narsi) Agaram
Rouba Ali-Fehmi
Ghassan Allo
Isabel Alvarado-Cabrero
Christina Arnold
Rohit Bhargava
Justin Bishop
Jennifer Boland
Elena Brachtel
Marilyn Bui
Shelley Caltharp
Joanna Chan
Jennifer Chapman
Hui Chen
Yingbei Chen
Benjamin Chen
Rebecca Chernock
Beth Clark
James Conner
Alejandro Contreras
Claudiu Cotta
Timothy D'Alfonso
Farbod Darvishian
Jessica Davis
Heather Dawson
Elizabeth Demicco
Suzanne Dintzis
Michelle Downes
Daniel Dye
Andrew Evans
Michael Feely
Dennis Firchau
Larissa Furtado
Anthony Gill
Ryan Gill
Paula Ginter
Tamara Giorgadze
Raul Gonzalez
Purva Gopal
Anuradha Gopalan
Jennifer Gordetsky
Rondell Graham
Alejandro Gru
Nilesh Gupta
Mamta Gupta
Krisztina Hanley
Douglas Hartman
Yael Heher
Walter Henricks
John Higgins
Mai Hoang
Mojgan Hosseini
Aaron Huber
Peter Illei
Doina Ivan
Wei Jiang
Vickie Jo
Kirk Jones
Neerja Kambham
Chiah Sui (Sunny) Kao
Dipti Karamchandani
Darcy Kerr
Ashraf Khan
Rebecca King
Michael Kluk
Kristine Konopka
Gregor Krings
Asangi Kumarapeli
Alvaro Laga
Cheng-Han Lee
Zaibo Li
Haiyan Liu
Xiuli Liu
Yan-Chun Liu
Tamara Lotan
Anthony Magliocco
Kruti Maniar
Jonathan Marotti
Emily Mason
Jerri McLemore
Bruce McManus
David Meredith
Anne Mills
Neda Moatamed
Sara Monaco
Atis Muehlenbachs
Bita Naini
Dianna Ng
Tony Ng
Ericka Olgaard
Jacqueline Parai
Yan Peng
David Pisapia
Alexandros Polydorides
Sonam Prakash
Manju Prasad
Peter Pytel
Joseph Rabban
Stanley Radio
Emad Rakha
Preetha Ramalingam
Priya Rao
Robyn Reed
Michelle Reid
Natasha Rekhtman
Michael Rivera
Michael Roh
Andres Roma
Avi Rosenberg
Esther (Diana) Rossi
Peter Sadow
Safia Salaria
Steven Salvatore
Souzan Sanati
Sandro Santagata
Anjali Saqi
Frank Schneider
Jeanne Shen
Jiaqi Shi
Wun-Ju Shieh
Gabriel Sica
Deepika Sirohi
Kalliopi Siziopikou
Lauren Smith
Sara Szabo
Julie Teruya-Feldstein
Gaetano Thiene
Khin Thway
Rashmi Tondon
Jose Torrealba
Evi Vakiani
Christopher VandenBussche
Sonal Varma
Endi Wang
Christopher Weber
Olga Weinberg
Sara Wobker
Mina Xu
Shaofeng Yan
Anjana Yeldandi
Akihiko Yoshida
Gloria Young
Minghao Zhong
Yaolin Zhou
Hongfa Zhu
Debra Zynger

299 Paragangliomas of Heart: Clinicopathologic and SHDB Immuniostainnstudy

Fadi Alakeel[1], Ghadah Al Sanna[1], Sergio Ibarra-Cortez[1], Michael Reardon[1], Bogdan Czerniak[2], Jae Ro[3]
[1]Houston Methodist Hospital, Houston, TX, [2]The University of Texas MD Anderson Cancer Center, Houston, TX, [3]Houston, TX

Disclosures: Fadi Alakeel: None; Ghadah Al Sanna: None; Sergio Ibarra-Cortez: None; Bogdan Czerniak: None; Jae Ro: None

Background: Paragangliomas (PGs) are rare neuroendocrine tumors originated from neural-crest-derived chromaffin cells. Around 35% of the PGs are inherited, and they are commonly associated with inherited syndromes including familial paraganglioma syndromes (FPSs). FPSs are commonly caused by germline mutations in succinate dehydrogenase (*SDH*) B, C, or D genes. *SDH* mutated PG has the potential to have an aggressive clinical course and a higher rate of recurrence, especially *SDHB* mutation. SDHB immunohistochemical (IHC) stain can be used as a surrogate marker to detect all *SDH* type mutations, as negative staining indicates that a high likelihood of mutations.
Cardiac PGs are exceedingly rare tumors representing < 1% of all cardiac tumors and <5% of all PGs. Genetic characterization and management guidelines are lacking due to the paucity of the cohort studies. This study aims to retrospectively assess the expression of SDHB in cardiac PG cases.

Design: This study includes patients diagnosed with cardiac PG at our institution from 1994 to 2017. Ten cases were identified, however; only 5 cases have tissue materials for SDHB IHC study. The diagnosis for all cases was made using the standard H&E and the available IHC stains including S100, chromogranin, and synaptophysin.

Results: Patient demographic information, tumor locations, and SDHB IHC stain results are summarized in table 1. IHC stain for SDHB is performed in 5 cases. One case showed a complete absence of SDHB IHC staining in the tumor cells (fig 1). The SDHB negative tumor is in a 34 years-old female and showed distinctive histologic features including nuclear atypia (fig 2A), focal necrosis (fig 2B), vascular invasion (fig 2C), and extensive transmural invasion extending to the endocardial and pericardial surfaces (fig 2A, 2D). The remaining four cases show weak to strong diffuse cytoplasmic staining pattern for SDHB IHC stain, and bland histology with no adverse histologic features.

Table 1. Demographic patients information and SDHB immunohistochemical (IHC) stain status.

	Age (years)/sex	Location	SDHB IHC Status
1	76/ female	Heart, not specified	Positive
2	34/ female	Heart, left atrium	Negative
3	62/ female	Heart, not specified	Positive
4	55/ male	Heart, left atrium	Positive
5	63/ male	Heart, left atrium	Positive
6	63/ male	Heart, septum	Not preformed
7	36/male	Heart, left atrium	Not preformed
8	35/ male	Heart, not specified	Not preformed
9	26/ male	Heart, posterior wall	Not preformed
10	69/ male	Heart, left atrium	Not preformed

Figure 1 - 299

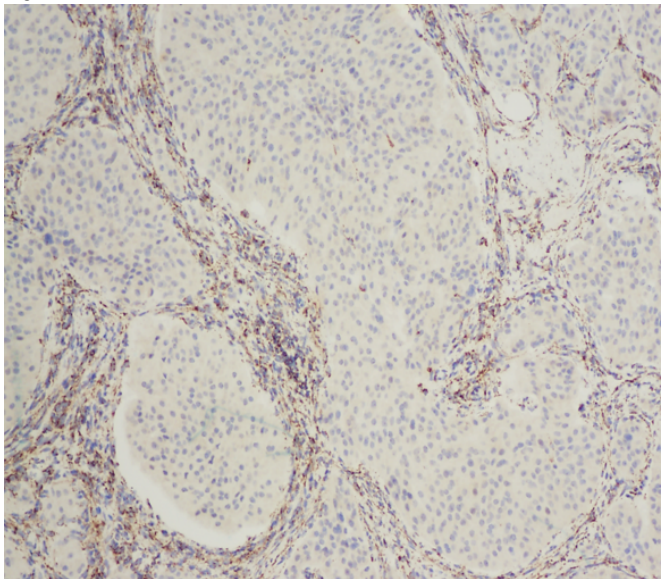

Figure 2 - 299

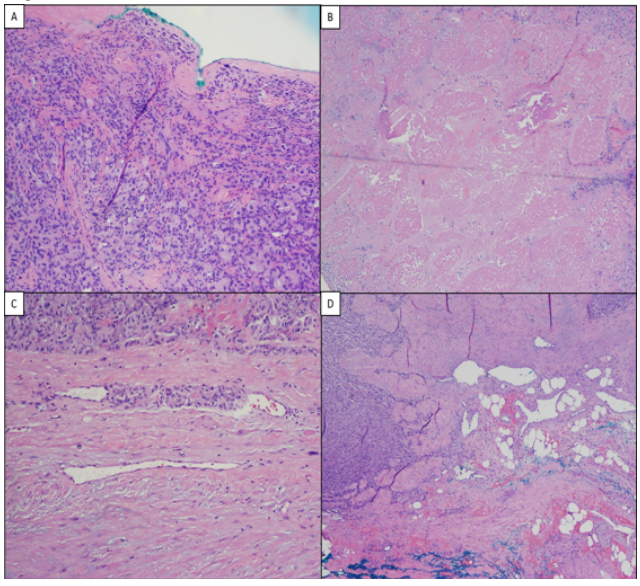

Conclusions: Cardiac PGs are extremely rare but have clinical importance due to their location; as they can interfere with heart functions. The commonest site is the left atrium as shown in our case series and other scattered case reports. Our results indicate that the case with negative SDHB IHC stain showed adverse histologic features including atypia, vascular invasion and endocardial/pericardial invasion. Therefore, identifying patients with *SDH* mutation by using the surrogate SDHB IHC stain marker will help in stratifying the risk in these patients.

300 Thickness of the Aortic Wall as a Predictor of Histological Damage in Patients with Bicuspid Valve Replacement: Study of 105 Cases

Maria Aon Bertolino[1], Alejandro Emilio Masucci[2], Mirian Matoso[3], German Gonzalez[2], Celina Morales[2]
[1]Federal Police Hospital, Lujan, Argentina, [2]Faculty of Medicine, Buenos Aires, Argentina, [3]National Judicial Morgue, Buenos Aires, Argentina

Disclosures: Maria Aon Bertolino: None; Alejandro Emilio Masucci: None; Mirian Matoso: None; German Gonzalez: None; Celina Morales: None

Background: Bicuspid aortic valve (BAV) is the most frequent congenital malformation with a prevalence of between 0.5% and 2% of the population. However, the relationship between BAVs, thickness (E) and the histological damage in aortic media layer (G) has not been sufficiently determinated.

Design: 105 patients operated on for bicuspid valve replacement with ascending aortas (AAs) diameter ? 40 mm were selected and measured by echocardiography between 2009 and 2017. 67% men; mean age of 53.5 ± 10.2 years and similar clinical conditions. Patients with Marfan´s Syndrome or other connective tissue abnormalities were not considered in this study. During valve replacement surgery, a sample of AAs was obtained from aortotomy area and fixed in 10% formaldehyde. Parietal thickness (E) was determinated with a caliper and then routine processed separated. H & E, Masson trichrome and Alcian blue staining for were performed. To establish the G, the histopathological findings of the intimal, adventitia and middle layer were studied (elastic fibers, collagen and smooth muscle, proteoglycans and inflammatory infiltrate) were studied in semi quantitative grade: G 0: without injury; G1: 0-10% (mild); G2: 11-25% (mild-moderate); G3: 26-50% (moderate); G4: 51-100% (severe). Thickness of the aortic wall ranges from 0 to 4 mm with interval of 0.5 mm. Statistical analysis was performed with simple frequencies and percentage distribution.

Results: For the total of 105 patients, 2.9% presented G0; 8.6% G1; 31.4% G2; 33.3% G3 and 23.8% G4. A statistically significant difference (p = 0.017) was found in the average aortic parietal thickness between the different degrees of pathological lesion. 88% of patients had aortic stenosis, within this group prevailed G2 (mild-moderate) and G3 (moderate). In contrast, in patients with aortic insufficiency, 82% had G3 (moderate) and G4 (severe).

Figure 1 - 300

TOTAL CASES (n)	GRADE OF LESION	% LESION	MEAN	MEDIAN	SD
3	0	2,9%	1,8667	1,8500	0,14572
9	1	8,6%	1,4878	1,2900	0,37036
33	2	31,4%	1,8473	1,8200	0,49246
35	3	33,3%	2,0309	2,0000	0,73595
25	4	23,8%	2,2544	2,0000	0,88842
105		100,00%			

Figure 2 - 300

105 AAs < 40mm

	Grade of injury					
Thickness interval mm	0	1	2	3	4	Total of patients
0-0,5			50%	50%		2%
0,51-1				50%	50%	2%
1,01-1,5		27%	36%	9%	27%	21%
E: 1,51-2	4%	6%	36%	40%	14%	48%
E: 2,01-2,5	13%	13%	25%	25%	25%	8%
E: 2,51-3			29%	29%	41%	16%
3,51-4				50%	50%	4%
Total	3%	10%	32%	31%	24%	100%

Conclusions: We could conclude the walls of the AAs of patients with bicuspid valves replacement without aortic dilation at the time of surgery showed a direct relationship between greater histological damage and greater parietal thickness (except in group 0), relevant findings that may have implications in the surgical treatment and the long term follow-up of patients.

301 Computational Histomorphometric Approach for Heart Transplant Rejection

Thomas Atta-Fosu[1], Andrew Janowczyk[1], Jeffrey Nirschl[2], Priti Lal[3], Michael Feldman[4], Eliot Peyster[3], Kenneth Margulies[3], Anant Madabhushi[1]

[1]Case Western Reserve University, Cleveland, OH, [2]Perelman School of Medicine at the University of Pennsylvania, Philadelphia, PA, [3]University of Pennsylvania, Philadelphia, PA, [4]University of Pennsylvania, Wilmington, DE

Disclosures: Thomas Atta-Fosu: None; Jeffrey Nirschl: None; Priti Lal: None; Michael Feldman: None; Kenneth Margulies: None; Anant Madabhushi: None

Background: Cardiac allograft rejection (CAR) is a serious concern in heart transplant medicine and requires vigilance to identify and treat. While morphologic analysis Cardiac allograft rejection (CAR) is a serious concern in heart transplant medicine and requires vigilance to identify and treat. While morphologic analysis of endomyocardial biopsy (EMB) samples using the International Society for Heart and Lung Transplantation (ISHLT) histologic grading scheme represents the standard in diagnosis for this syndrome, this standard has limitations in precision and accuracy that directly affect patient care. An unbiased automated approach to histomorphometric rejection grading has the potential to serve as a valuable clinical decision support tool and a highly reliable standard for inter-facility research and collaboration. As part of developing such an approach, we sought to explore whether automated identification and quantification of lymphocyte infiltrates – the foundation of the ISHLT grading schema – can be used to accurately classify low-histologic grades (0R-1R) vs high histologic grades (2R-3R)

Design: A total of 1136 biopsy instances from 410 heart transplant patients with histologic grading between 0R(no rejection) and 3R (severe) were analyzed. We use baseline quantitative descriptors to encode the extent of lymphocyte infiltrate foci on EMBs at 20x magnification. Foci of Lymphocyte infiltrate is segmented from image patches, followed by morphologic processing to excluded false lymphocyte foci. The total count of foci, and the ratio of foci to tissue area aggregated over patches extracted from the biopsy images are used as features. We use a multi-layer perceptron with 2 hidden layers, with 5 and 10 units respectively, for binary classification of the four grades into low grade (0R, 1R) and high grade (2R, 3R). We use 70% of the EMBs for training, and the remaining 30% for independent validation.

Results: We record an accuracy of 87% on the independent validation, and an area under ROC curve of 0.93. We also record precision and recall of 81% and 79% respectively.

Table 1: A summary of composition of rejection grades and the associated biopsy samples

Grade 0R	Grade 1R	Grade 2R	Grade 3R
309	453	316	58

Figure 1 - 301

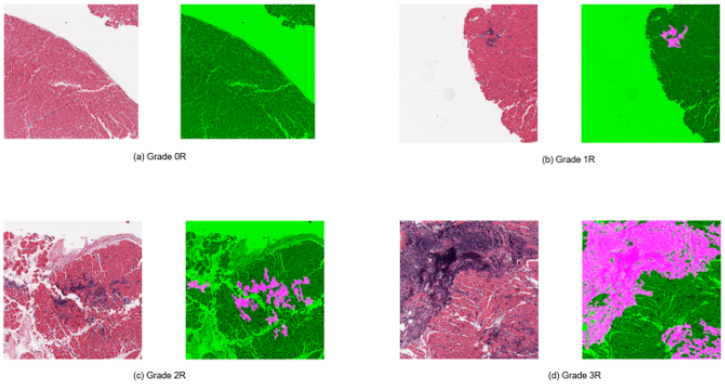

Fig 1. Results of the lymphocyte infiltration foci detection on sample grade 0R image – (a), grade 1R – (b), grade 2R (c), and grade 3R – (d). The left panels in the subplots show the input patches from H&E images. In the right panels, the detected lymphocyte foci (purple) are superimposed. Lymphocyte focus that do not meet a size threshold is masked out - including individual lymphocytes, with masked out regions shown as green background in the right panels.

Figure 2 - 301

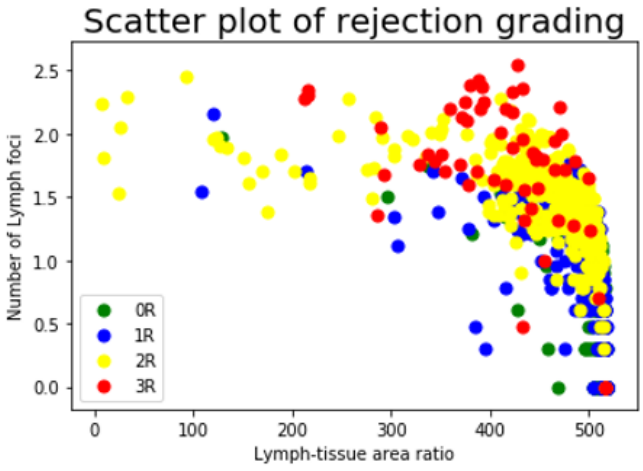

Fig 2. A scatter plot of the two biopsy samples using the two infiltrate derived quantitative features.

Conclusions: The area and number of lymphocyte foci in a biopsy can independently predict heart transplant rejection grade when rejection grades are binarized into low and high grade.

302 Absence of KRAS Mutations in Lambl Excrescences: A Cohort Suggesting Distinct Pathogenic Mechanisms from Papillary Fibroelastoma

Melanie Bois[1], Catherine Morris[1], Dragana Milosevic[1], Benjamin Kipp[1], Joseph Maleszewski[1]
[1]Mayo Clinic, Rochester, MN

Disclosures: Melanie Bois: None; Catherine Morris: None; Dragana Milosevic: None; Benjamin Kipp: None; Joseph Maleszewski: None

Background: Lambl excrescences (LEs) are filiform projections commonly found on aortic valves, particularly in older individuals. Their resemblance to papillary fibroelastoma (PFE) has led to the notion that the two lesions may exist on a spectrum, with PFE representing a "giant" form of LE. Nevertheless, important differences in occurrence site have been observed, arguing against a common etiology. Until recently, the paucicellularity of these lesions has precluded a detailed survey of the molecular biology of these lesions. Advances in digital droplet polymerase chain reaction (ddPCR) have shown that a subset (approximately 25%) of PFEs to harbor activating *KRAS* mutations, though the LE has hitherto not been similarly evaluated. Molecular interrogation of a cohort of LEs was undertaken to evaluate for *KRAS* gene status.

Design: LEs were prospectively identified on surgical resected aortic valves (2/22/2018-6/22/2018) and wholly isolated for DNA extraction. Relevant clinical information was abstracted from the medical record. Extracted DNA was subjected to ddPCR and analysis for common *KRAS* mutations (codons 12, 13 and 61). Given the paucicellularity of these lesions, any mutant DNA copies were considered as a potential positive result.

Results: 20 LEs (0.2-0.5 cm) were identified (19 from aortic valves, 1 from a pulmonary homograft). Median patient age was 72 years (interquartile range 64-78 years); 14 (70%) were men. The most common underlying pathology was degenerative fibrocalcific aortic valve disease (n=15; 75%), followed by congenitally bicuspid aortic valves (n=2; 10%), and one each of post-inflammatory valve disease, partial aortic valve cusp excision during septal myectomy for "mass-like" lesions, and pulmonary homograft revision. Although overall DNA recovery was low, no mutant droplets were detected.

Conclusions: LEs do not appear to harbor *KRAS* mutations in common areas of the gene that have been implicated in the pathogenesis of PFEs. This observation has two potential implications: 1) it provides evidence that indeed the LE is a separate and distinct pathological

process from that of PFE. 2) LEs appear to be non-neoplastic in nature and thus may be reactive of degenerative phenomena. The study is limited both by cohort size as well as the overall low cellularity of the tested lesions.

303 PDE11A and PRKAR1A Expression in Cardiac Myxomas

Melanie Bois[1], Rondell Graham[1], Joseph Maleszewski[1]
[1]Mayo Clinic, Rochester, MN

Disclosures: Melanie Bois: None; Rondell Graham: None; Joseph Maleszewski: None

Background: Phosphodiesterase 11A (PDE11A) and the 1-alpha regulatory subunit of protein kinase A (PRKAR1A) both serve to regulate cytoplasmic cyclic (c)AMP. Inactivating mutations in both *PDE11A* and *PRKAR1A* have been implicated in CNC-associated adrenal and testicular lesions. Inactivation of PRKAR1A has also been well documented in cardiac myxomas associated with Carney complex (CNC), although the role for PDE11A has yet to be established. A cohort of cardiac myxomas was evaluated for both PRKAR1A and PDE11A expression, with subsequent molecular genetic analysis of both genes.

Design: Surgical pathology archives were queried for cases of cardiac myxoma (2011-2016). PDE11A (Sigma-Aldrich, St. Louis MO USA) and PRKAR1A (OriGene, clone OTI6C7, Rockville, MD) immunohistochemistry (IHC) was performed on formalin-fixed, paraffin embedded (FFPE) tissue sections and scored for intensity in a semiquantitative fashion (0-2). Next generation sequencing of nucleic acids, extracted from FFPE myxoma specimens, was performed to specifically evaluate *PDE11A*. Variant classification was performed according to American College of Medical Genetics guidelines. Salient clinical information was abstracted from the medical record.

Results: 20 patients (13 women) were identified (median age, 75 years; interquartile range 61-80 years). 6 (30%) patients demonstrated no PRKAR1A staining within the lesional cells. Of these, 2 cases showed diffuse/strong PDE11A expression and 4 cases demonstrated faint/granular expression. Remaining cases showed faint/granular PRKAR1A immunoreactivity in 2 (10%) cases and strong/diffuse in 12 (60%) cases. All cases with retained PRKAR1A expression showed faint/granular PDE11A immunoreactivity. No cases showed loss of PDE11A immunoreactivity. PRKAR1A-deficient myxomas demonstrated increased expression of PDE11A (p=0.02). No definitive pathogenic mutation in *PDE11A* been identified, although analysis is ongoing.

Conclusions: Upregulation of PDE11A is present in PRKAR1A-deficient myxomas. This compensatory activity implicates cytoplasmic cAMP accumulation as a driver of tumorigenesis in cardiac myxoma, and suggests a role of PDE11A in myxoma pathogenesis. Although no pathogenic *PDE11A* mutation has been documented to date, continued investigation of its role as a molecular driver in cardiac myxoma is warranted.

304 Immune Checkpoint Inhibitor Associated Myocarditis Occurs in Distinct High-Grade and Low-Grade Forms

Samantha Champion[1], James Stone[2]
[1]Massachusetts General Hospital, Boston, MA, [2]Massachusetts General Hospital, Charlestown, MA

Disclosures: Samantha Champion: None; James Stone: None

Background: Immune checkpoint inhibitor (ICI) therapy for malignancy has been associated with adverse events including myocarditis. It has been unclear if there are distinct pathologic grades of immune checkpoint inhibitor associated myocarditis (ICIM) and if such grades are associated with distinct clinical outcomes.

Design: Cardiac tissue from 6 patients with ICIM (5 biopsies and 1 autopsy) were evaluated using immunohistochemistry for CD3, CD8, CD68, tryptase, PD-L1 and C4D. The numbers of cells staining in the 10 400X hpfs with the most inflammation were counted, and the data expressed as cells/hpf (mean±SE). The cases were divided into two groups based on the density of CD3+ T-cells: high-grade ICIM (H-ICIM, >50 CD3+ cells/hpf) or low-grade ICIM (L-ICIM, ≤50 CD3+ cells/hpf). The densities of macrophages, T-cells, mast cells, eosinophils, necrotic myocytes and PD-L1+ macrophages and myocytes were compared between the two groups, as were the interval from first ICI treatment, serum troponin level, left ventricular ejection fraction (LVEF), and survival. Two patients had been treated with nivolumab, two with pembrolizumab, and two with nivolumab/ipilimumab.

Results: Three patients were classified as H-ICIM and three as L-ICIM. There was no difference between the two groups in the density of tryptase positive mast cells (2.0±0.5 vs 2.3±0.4 cells/hpf) or of PD-L1+ macrophages (1.7±0.6 vs 1.4±0.6). Compared with L-ICIM, in the H-ICIM group there were marked trends toward increased numbers of CD3+ T-cells (111±33 vs 14±6), CD8+ T-cells (58±26 vs 12±6), eosinophils (1.6±1.6 vs 0.03±0.03), necrotic C4D+ myocytes (15±10 vs 0.13±0.09), and PD-L1+ myocytes (2.6±1.7 vs 0.33±0.15). There was a statistically significant higher density of CD68+ macrophages in the H-ICIM group compared with the L-ICIM group (81±21 vs 8.8±1.4, P=0.004). In the H-ICIM group, there was a modest trend towards lower LVEF (51±8% vs 62±7%), a marked trend toward shorter interval from first ICI treatment (27±5 vs 371±212 days), and significantly higher serum troponin levels (1.4±0.5 vs 0.036±0.021 ng/mL, P=0.0049). All the patients with H-ICIM died, while all the patients with L-ICIM were still living.

Conclusions: ICIM occurs in two distinct forms, a high-grade form (H-ICIM) with a more fulminant clinical course, and a low-grade form (L-ICIM) with a more indolent clinical course. In this initial small group of patients with ICIM, a cutoff of 50 CD3+ cells/400x hpf was adequate to delineate these two forms of the disease.

305 HPA and HPASubC Identify the Proteome of Cardiac t-Tubules

Jenice Cheah[1], Tim Nieuwenhuis[1], Marc Halushka[1]
[1]Johns Hopkins University School of Medicine, Baltimore, MD

Disclosures: Jenice Cheah: None; Marc Halushka: None

Background: Transverse tubules (t-tubules) are important structural elements, derived from sarcolemma, found on all striated myocytes. These specialized organelles create a scaffold for many proteins crucial to the effective propagation of signal in cardiac excitation-contraction coupling. The full protein composition of this region is unknown.

Design: We characterized the t-tubule subproteome using 52,033 immunohistochemical images covering 13,203 proteins from the Human Protein Atlas (HPA) cardiac tissue microarrays. We used HPASubC, a suite of Python tools, to rapidly review and classify each image for a specific t-tubule staining pattern. The tools Gene Cards, String 10.5, and Gene Ontology (GO) Consortium as well as literature searches were used to understand pathways and relationships between the proteins.

Results: There were 96 likely t-tubule proteins discovered by HPASubC. Of these, 12 were matrisome (extracellular matrix) proteins and 3 were mitochondrial proteins. A separate literature search identified 54 t-tubule proteins. A comparison of those lists revealed only 17 proteins in common, including 8 of the matrisome proteins. For the 81 HPASubC t-tubule proteins, in a query for biological process, the top GO terms were “caveola assembly”, “receptor-mediated endocytosis of a virus by host cell” and “protein localization to a membrane raft.” String10.5 revealed that 37 of the 80 proteins generated a single interconnected network.

Conclusions: We identified 78 novel, putative t-tubule proteins that expands and improves our knowledge of this important subcellular structure of the cardiac myocyte using HPASubC and the HPA. This information can be used to identify new structural targets involved in excitation-contraction coupling that may be altered in disease.

306 Left Dominant Arrhythmogenic Cardiomyopathy: an Emerging Cause of Sudden Death

Monica De Gaspari[1], Stefania Rizzo[2], Gaetano Thiene[2], Kalliopi Pilichou[1], Cristina Basso[3]
[1]University of Padua, Padua, Italy, [2]University of Padua, Padova, Italy, [3]University of Padua Medical School, Padova, Italy

Disclosures: Monica De Gaspari: None; Stefania Rizzo: None; Gaetano Thiene: None; Kalliopi Pilichou: None; Cristina Basso: None

Background: Arrhythmogenic cardiomyopathy (AC) is a genetically determined heart muscle disease characterized by progressive myocardial atrophy with fibro-fatty substitution. In the recent years, besides classical right ventricular (RV) and biventricular variant (BiV), a dominant or isolated left ventricular (LV) variant has been increasingly recognized by either histology or contrast enhanced cardiac magnetic resonance.

Design: To assess the prevalence and electrocardiographic (ECG) and pathologic characteristics of LV AC variant in our AC collection of heart specimens. We reviewed the AC heart specimens and histologic slides of: a) 74 juvenile SD (50 M, mean age 26 years); b) 33 cardiac transplantation – CT (18 M, mean age 45 years). For each case, we looked for type of involvement (RV, BiV or LV) and other gross and histological features and ECG tracings when available.

Results: A total of 20 (19%) LV variant are identified, vs 14 (13%) RV and 72 (67%) BiV. In the SD group, LV variant was detected in 18 (24%) of AC cases, while in the CT group it was detected only only in 2 (6%). In both groups the majority of AC were BiV (58% in the SD and 88% in the CT group).

At histology, the LV variant showed fibrous replacement in 4 (22%) cases of the SD group and 1 (50%) of the CT group, whereas fibro-fatty replacement was present in 14 (78%) SD cases and 1 (50%) CT case. The extent of fibrous/fibro-fatty replacement was transmural in 2 (10%) of LV vs of 14 (100%) RV and 41 (94%) of BiV variants ($p < 0,001$ LV vs other).

ECG was available in 13 LV, 8 RV and 49 BiV variants. In the LV variant subgroup, ECG features consisted of normal ECG in 69% (vs 37% in RV and 45% in BiV), inverted T waves in precordial leads in 0, inverted T waves in lateral leads in 3 (23%), low voltage QRS in 2 (15%).

Genetic testing was performed in 8 LV, 2 RV and 37 BiV and resulted positive for known AC pathogenic mutations in 4 LV (50%), 2 RV (100%) and 24 BiV (65%).

Conclusions: Left dominant AC is increasingly recognized as a cause of SD representing one fourth of juvenile SD cases due to AC. In these cases, the free wall involvement is only exceptionally transmural and never accounting for wall thinning, aneurysms formation or chamber dilatation. ECG tracing is normal in more than two thirds of cases. Our data explain why clinical diagnosis of LV AC variant remains challenging in the absence of diagnostic tools allowing tissue characterization.

307 Radiofrequency Catheter Ablation of Atrial Flutter: Interventional Anatomy of the Cavo-Tricuspid Isthmus

Monica De Gaspari[1], Stella Bacillieri[2], Stefania Rizzo[3], Beatrice Paradiso[4], Gaetano Thiene[3], Roberto Verlato[2], Cristina Basso[5]
[1]University of Padua, Padua, Italy, [2]Camposampiero Hospital, Camposampiero, Italy, [3]University of Padua, Padova, Italy, [4]University of Padua Medical School, Padua, Italy, [5]University of Padua Medical School, Padova, Italy

Disclosures: Monica De Gaspari: None; Stella Bacillieri: None; Stefania Rizzo: None; Beatrice Paradiso: None; Gaetano Thiene: None; Cristina Basso: None

Background: Radiofrequency (RF) catheter ablation a common therapeutic strategy for cavo-tricuspid isthmus (CTI)-dependent atrial flutter (AFL). Our aim was to assess the rate of complications and the role of right atrial CTI morphology in the success of RF catheter ablation for CTI-dependent AFL.

Design: Angiographically-determined CTI morphology was classified as simple or complex (with pouch-like recesses) in 337 patients with RF catheter ablation for CTI-dependent AFL. A series of 104 consecutive autopsy hearts was examined for morphology assessment of the CTI variants.

Results: Complex CTI anatomy was present in 11% of AFL cases. In these patients, the time of RF application to achieve bidirectional isthmus block was longer (57.3 vs 50.4 min). Acute procedure failure or major complications occurred in 3 cases, all with complex CTI anatomy.

A total of 10% of autopsy hearts presented sub-Eustachian recesses. The recess was single in the majority of cases (60%) and the most frequent location was the central isthmus (60%). Histomorphometric analysis of the CTI atrial wall thickness demonstrated that the anterior, the middle paraseptal and middle central regions were the thinnest ones (mean 0.9, 1.0 and 1.0 mm respectively).

Conclusions: RF catheter ablation is a safe and effective therapy for AFL. Knowledge of the morphological variants of the CTI region could improve the procedural technique and prevent possible complications.

308 BRG1 as a Potential Diagnostic Immunohistochemical Marker for Hypertrophic Obstructive Cardiomyopathy

Carolyn Glass, Duke University Medical Center, Durham, NC

Disclosures: Carolyn Glass: None

Background: Hypertrophic obstructive cardiomyopathy (HOCM) may be defined histologically by features such as myocyte disarray, interstitial fibrosis, and vascular smooth muscle hyperplasia. To date, a specific immunohistochemical (IHC) biomarker for HOCM is not available. IHC may particularly be helpful in confirming diagnosis in patients with a clinical diagnosis of HOCM but absent typical histologic features due to limited sampling or other factors. Recent landmark animal studies (Hang, Nature 2010) show BRG1, a subunit of the chromatin modifying SWI/SNFcomplex, is activated during normal fetal cardiac development, repressed in normal adult hearts, and reactivated in the setting of HOCM due to transcriptional reprogramming. Here we show BRG1 is reactivated in *human* adult cardiomyocytes in patients with clinical HOCM, supporting its use as a possible diagnostic biomarker.

Design: A cohort of 78 human cardiac specimens between 2008-18 (30 HOCM, 10 DCM, 10 with left ventricular hypertrophy secondary to other etiology, 20 normal fetal hearts and 8 normal adult autopsy hearts) were included from a high volume academic cardiac transplant center. IHC was performed in normal fetal and adult human hearts to map the natural course of BRG1 expression during normal cardiac development. BRG1 expression was then scored (0=no expression, 1=minimal, 2=moderate, 3=strong) in HOCM hearts and the appropriate normal and diseased controls. Expression levels were correlated with gross and microscopic findings. <

Results: BRG1 nuclear expression was diffusely strong in developing fetal hearts (range 2 to 3, mean 2.5) up to age 24 weeks. A sharp decline to near complete loss of expression (mean 0.08, $p<0.0001$) occurred at 25 weeks which was sustained throughout adulthood (mean 0.31). BRG1 nuclear expression was significantly greater in HOCM adult cardiac myocytes (range 1.5 to 3, mean 2.07) compared to DCMas well as other disease states resulting in left ventricular hypertrophy (range 0 to 1.5, mean 1.21, $p<0.01$). BRG1 expression in HOCM myocytes was similar to expression levels found in normal developing fetal hearts, but significantly greater than normal adult hearts (range 0 to 1, mean 0.313, p=<0.0001).

Figure 1 - 308

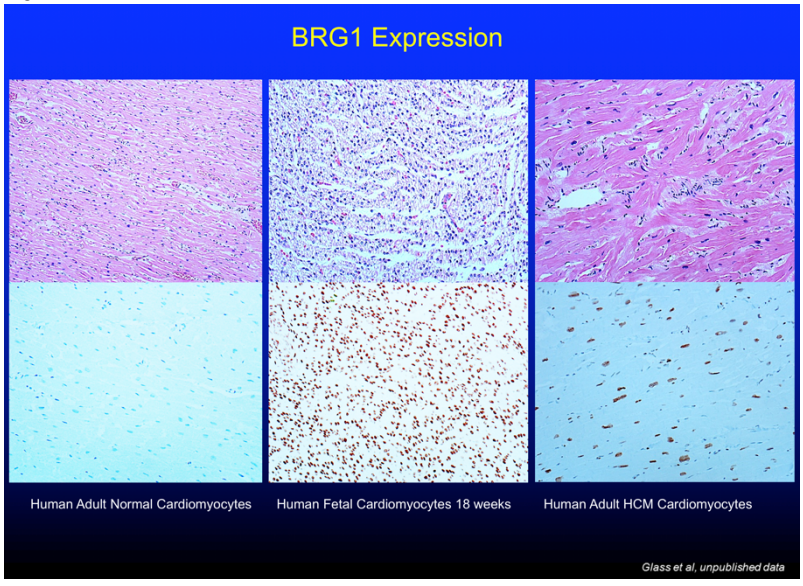

Conclusions: This study supports reactivation of BRG1 occurs in HOCM human hearts, supporting in part a mechanism that switches the adult heart back to a fetal molecular signature. More importantly, based on this pilot study BRG1 may potentially be used as one of the first IHCs to diagnose HOCM in biopsies and explanted hearts.

309 Differential Expression of NUP98-ERBB4-PSEN1-NRG1 (NEPN) Signaling Axis as Potential Blood-Based Biomarker for Viral Myocarditis

Paul Hanson[1], Veena Lin[1], Bruce McManus[2]
[1]University of British Columbia, Vancouver, BC, [2]University of British Columbia and St. Paul's Hospital, Vancouver, BC

Disclosures: Paul Hanson: None; Veena Lin: None; Bruce McManus: None

Background: Myocarditis, inflammation of the myocardium, is a leading cause of unexpected heart failure in young adults, commonly attributable to viral infections. Myocarditis manifests in a wide range of clinical presentations, from asymptomatic to acute heart failure. The current gold standard for diagnosis relies upon invasive endomyocardial biopsy, requiring histopathological demonstration of inflammation with/without associated myocyte damage. Under these guidelines, diagnostic sensitivity in independent published studies is <30%. We have previously demonstrated that detection of biomarkers within the NEPN pathway (implicated in immune response and heart failure) significantly improved diagnostic sensitivity to ~80%, however, this approach still relies upon biopsy. Thus, in the present study, our aim is to develop a non-invasive, blood-based diagnostic assay for viral myocarditis by examining the NEPN signaling axis and their cleavage fragments during the evolution of myocarditis.

Design: HeLa cells and human induced pluripotent stem cell (iPSC)-derived cardiomyocytes (CM) were CVB3- or sham-infected. Western blot analysis and confocal microscopy were performed to determine the expression and subcellular localization of NEPN signaling axis proteins in tissue culture. In addition, tissue and blood from murine models of viral myocarditis (A/J and C57BL/6 mice) were collected at 4 dpi (viremic phase) and 5 to 8 dpi (acute phase), and were analyzed by Western blot analysis, IHC and IF to detect protein expression.

Results: NEPN proteins all show changes in expression and subcellular localization throughout the infection time course. NUP98 is upregulated and cleaved during infection. NRG1 is upregulated in both lysates and supernatants. ERBB4 co-localizes at the cell membrane with the protease PSEN1. ERBB4 and NRG1 cleavage fragments are secreted and detected in both tissue culture supernatant and mouse plasma. In the plasma of the less susceptible C57BL/6 mice, ERBB4 and NRG1 cleavage fragments increase throughout the viremic and acute phases. However, in the highly susceptible A/J mice, ERBB4 and NRG1 cleavage fragments were not detected in the plasma until 6 dpi (acute phase), when they are highly upregulated as compared to C57BL/6 mice (p=0.001).

Conclusions: Differential expression, subcellular localization and cleavage fragments of NEPN signaling axis proteins were detected during the pathogenesis of viral myocarditis. These composite changes may be useful in the development of a blood-based diagnostic

310 Intimal sarcoma is the most frequent primary pulmonary sarcoma not in cardiac sarcoma: Clinicopathologic and molecular feature of primary cardiac and pulmonary artery sarcomas

Li Li, Fuwai Hospital, Chinese Academy of Medical Sciences, Beijing, China

Disclosures: Li Li: None

Background: Neoplasms arising in the heart or the large vessels are rare. There are few series describing sarcomas of the heart and pulmonary, espically on the histological features. Up to date, the intimal sarcoma in heart have been reported by some authors, although there is a substantial divergence of existence of intimal sarcoma in heart. The difference of histological and molecular features, prognostic and tailored therapeutic biomarkers of cardiac and pulmonary intimal sarcoma are lacking. In the present study, we performed a study of 33 cases of these sarcomas.

Design: The tumor tissues were analyzed by histopathology, immunohistochemistry. For all the cases positive with MDM2, fluorescence in situ hybridization (FISH) was carried out. All tumors were classified and graded according to the Armed Forces Institute of Pathology classification and FNCLCC grading system. The immunohistochemical stainings used the following antibodies: platelet-derived growth factor receptor α (PGDFRA), epidermal growth factor receptor (EGFR) and MDM2. MDM2 positive nuclei were counted and expressed as percentage of total cell number. MDM2 positive cell percentage was considered high when higher than 20%. Follow-up data was obtained by contacting the patient or patient's family.

Results: Of 33 patients, 17 tumors were cardiac tumors and 16 tumors were pulmonary sarcomas. The most common histologic types in cardiac sarcomas were angiosarcoma (n=6) and intimal sarcoma (IS, n=4). Pulmonray sarcomas were classified as intimal sarcoma (n=10),undifferentiated pleomorphic sarcoma(UPS, n=2), myxofibrosarcoma (n=1), osteosarcoma (n=1) and chondrosarcoma (n=2). Higher levels of MDM2 immunostaining were seen mainly in pulmonary IS (49.1±18.5 vs 3.6±2.9, p=0.04). High levels of MDM2 gene amplification were also seen in pulmonary IS. EGFR were expressed in 90% of pulmonary IS and in 25% of cardiac IS. PDGFRA was expressed in 50% of pulmonary IS lesions and 25% of cardiac IS. Follow-up revealed that 7 of 8 patients with pulmonary IS died (n=4) or recurred (n=3) within 6 months, one patient was alive to end of follow-up for 3 months. Three of 4 patients with cardiac IS survived more than one year.

Conclusions: Intimal sarcoma is the most common type of pulmonary artery sarcoma not in cardiac sarcoma. Pulmonary IS and cardiac IS showed different MDM2 expression levels both on gene and protein levels and were characterized by different prognosis.

311 Valvular Serotonin (5-HT) Receptor Expression in Carcinoid Heart Disease

Catherine Morris[1], Elizabeth Cheek[1], Sarah Jenkins[1], S. Allen Luis[1], Patricia Pellikka[1], Heidi Connolly[1], Joseph Maleszewski[1], Melanie Bois[1]
[1]Mayo Clinic, Rochester, MN

Disclosures: Catherine Morris: None; Elizabeth Cheek: None; Sarah Jenkins: None; S. Allen Luis: None; Patricia Pellikka: None; Heidi Connolly: None; Joseph Maleszewski: None; Melanie Bois: None

Background: Carcinoid heart disease (CHD) is characterized by valvular thickening caused by myofibroblastic plaques thought to be driven by high circulating serotonin levels. The striking predilection for the right-sided valves is thought to be due to serotonin inactivation in the lungs, thereby sparing the left-sided cardiac structures. Recently, however, plasma levels of serotonin were shown to be similar in the left- and right-sided cardiac chambers of patients with carcinoid syndrome, calling this mechanism into question. To this end, immunohistochemical (IHC) evaluation of serotonin receptors in left- and right-sided valves was undertaken to assess for site-specific differences in the receptor biology.

Design: Surgical pathology and autopsy databases were queried for cases of CHD (1997-2016). Cases were selected based on availability of multiple valves for evaluation. Controls were prospectively procured from autopsy patients with no cardiac disease. Five immunohistochemical antibodies to various serotonin receptors (5-HT1B, 5-HT2B, 5-HT4; Sigma-Aldrich, St. Louis, MO, 5-HT1D; Novus Biologicals, Littleton, CO and 5-HT2A; Antibodies-online, Atlanta, GA) were optimized. Distribution (0-3) and intensity (0-2) of staining of the valvular interstitial cells was semiquantitatively assessed. A combined histochemical score, the product of distribution and intensity scores, was recorded.

Results: 24 patients and 19 controls were included. Within the carcinoid group, 5 (21%) cases had isolated right-sided disease, 15 (62%) had both right- and left-sided disease and 4 (17%) had left-sided disease only. Serotonin expression is summarized in the Table. 5-HT2A expression was significantly higher among CHD valves as compared to control cases ($p<0.0001$). No difference was seen on pairwise analysis within the case cohort or control cohort.

Table. Serotonin receptor H-Score by Valve

	5-HT1B			5-HT1D			5-HT2A			5-HT2B			5-HT4		
	CHD	Control	P-value	CHD	Control	P-value	CHD	Control	P-value	CHD	Control	P-value	CHD	Control	P-value
Tricuspid[1]	3.1	3.8	0.4606	3.0	2.6	0.1777	3.3	0.5	<0.0001	6.0	5.4	0.889	5.5	5.1	0.5443
Pulmonary[2]	2.5	3.9	0.0022	3.0	3.1	0.8538	3.2	0.7	<0.0001	5.6	5.8	0.5880	4.9	5.6	0.2167
Mitral[3]	3.0	3.5	0.3365	2.6	2.7	0.7134	2.5	0.5	<0.0001	5.0	5.3	0.5507	4.5	4.7	0.7357
Aortic[4]	2.9	3.8	0.0599	2.8	2.8	0.7727	2.3	0.7	<0.0001	5.8	5.7	0.7242	5.1	5.2	0.9101

[1]CHD n=18, control n=19; [2]CHD n=17, control n=16; [3]CHD n=13, control n=19; [4]CHD n=15, control n=19

Conclusions: No significant difference in serotonin receptor IHC was seen in right-sided versus left-sided valves, questioning the exclusive role of serotonin in the development of CHD. Nevertheless, 5-HT2A demonstrates significantly greater expression in patients than controls, suggesting (at least) upregulation of 5-HT2A in patients with CHD and a potential therapeutic target. Investigations into the role this receptor plays in the propagation of CHD is ongoing.

312 Hypertrophic Cardiomyopathy: Genotype-Phenotype Correlation of 14 Autopsy Cases

Catherine Morris[1], Linnea Baudhuin[1], Melanie Bois[1], Joseph Maleszewski[1]
[1]Mayo Clinic, Rochester, MN

Disclosures: Catherine Morris: None; Linnea Baudhuin: None; Melanie Bois: None; Joseph Maleszewski: None

Background: Hypertrophic cardiomyopathy (HCM) is a primary disorder of the cardiac sarcomere with a wide spectrum of presentation, ranging from asymptomatic to sudden death. It affects approximately 1 in 500 people and has been linked to multiple genomic alterations. In this study, we present 14 cases of HCM with detailed gross, histological, and molecular genetic findings.

Design: Institutional archives were queried for cases of hypertrophic cardiomyopathy autopsied between 2009 and 2015. Detailed cardiac gross findings were abstracted from the pathology reports, and where possible, archived wet tissue was reviewed. Histologic sections were also reviewed. Extracted DNA was sequenced on the Illumina MiSeq with utilization of Agilent SureSelect targeted capture of 54 genes associated with cardiomyopathies. Identified variants were subsequently classified according to established American College of Medial Genetics (ACMG) guidelines and paired with their respective gross and histologic features.

Results: 14 total cases were identified, including 9 men and 5 women (age range, 16-74 years). Cardiac weight averaged 121% above the expected mean based on the decedent's body size. Average left ventricular free wall thickness was 1.4 cm, with an average septal to free wall ratio of 1.3:1. Residual wet tissue was available in 9 cases. Among these, the mean anterior mitral valve length was 2.0 cm (1.7-2.5 cm); subendocardial contact lesions were observed in 75%. No papillary muscle or cord anomalies were noted. Clinically significant variants were identified in 11 cases, with 2 containing pathogenic variants and 12 containing variants of undetermined significance.

Age/Sex	Cardiac Weight (g)	Expected[1] Cardiac Weight (g)	IVS:LVFW Ratio[2]	Disarray[3]	Fibrosis[3]	Nuclear Hypertrophy[3]	Genetic Variants[4]
56/F	760	237	1.1	2	3	3	*MYBPC3* (P), *TTN* (VUS)
46/M	730	349	1.3	1	2	3	*TTN*(VUS), *PKP2*(VUS), *RBM20*(VUS)
71/M	660	318	1.5	1	2	3	None
19/M	540	308	1.4	1	2	2	None
45/M	750	349	1.6	1	3	3	*LDB3* (VUS), *TTN*(VUS)
56/F	782	253	1.0	2	3	3	*VCL*(VUS)
16/F	352	284	1.0	2	1	3	*MYH7* (P)
70/F	592	244	1.2	2	3	3	*RYR2*(VUS)
51/M	561	314	1.4	2	1	2	*RBM20*(VUS)
49/M	500	330	1.5	1	1	3	*TTN*(VUS), *MYPN*(VUS)
72/F	800	266	1.1	2	3	3	*MAP2K1*(VUS)
50/M	672	353	1.0	1	2	3	*TTN*(VUS)
74/M	937	324	1.0	2	2	2	None
71/M	504	284	1.6	2	3	3	*MYBPC3*(VUS)

[1]Expected cardiac weight was calculated based on the height.

[2]Intraventricular septum (IVS): left ventricular free wall ratio (LVFW) ratio.

[3]Myocardial fiber disarray, fibrosis and nuclear hypertrophy were assessed on a scale of 0-3.

[4] (P) –Pathogenic & (VUS) – Variant of uncertain significant.

Conclusions: A spectrum of gross, histologic and molecular genetic findings exists for hypertrophic cardiomyopathy. No single morphological (gross or histologic) feature appears to be predictive of the presence of an underlying molecular genetic abnormality or a specific genotype, in this series. The study is limited by a lack of an objective diagnostic gold-standard for hypertrophic cardiomyopathy as well as the relatively small size of the cohort. Additional work is necessary to expand the cohort and explore additional potential genotype-phenotype correlations.

313 Healed Arteritis – Retrospective Review of Temporal Artery Biopsies

Atsuko Seki[1], Carmela Tan[1], E. Rene Rodriguez[1]
[1]Cleveland Clinic Foundation, Cleveland, OH

Disclosures: Atsuko Seki: None; Carmela Tan: None; E. Rene Rodriguez: None

Background: Examination of temporal artery biopsies may show minimal to no inflammation but evidence of vessel damage. Criteria to differentiate between post-inflammatory injury versus arteriosclerosis are poorly defined, thus making a consistent diagnosis of healed arteritis (HA) difficult. Our aim is to characterize and validate histological patterns of HA and determine its incidence and clinical implications in a single-center study.

Design: There were 1189 temporal artery biopsies performed from 01/2006 to 08/2018. Biopsies initially reported as HA or suggestive of HA were re-reviewed together by the three authors to establish a consensus diagnosis. Orientation of the specimen, periarterial compartment, tunica adventitia, media and intima were systematically evaluated. The electronic medical record was reviewed to evaluate for treatment decision after the diagnosis of HA.

Results: There were 63 out of 1189 biopsies from 62 patients (1 patient had bilateral biopsies) with histologic features consistent with or suggestive of HA. Thirty of 63 biopsies (48%) were reclassified as HA. The frequency of the different histologic features observed were as follows: loss of the internal elastic lamina (IEL) (30/30 biopsies =100 %), medial replacement fibrosis (30/30 = 100%), irregular intimal thickening (23/30 = 77%), presence of inflammatory cells (15/30 = 50%; adventitia:12/30 = 40%, small vessels: 5/30 = 17%),

neovascularization (7/30 = 23%). Tangential sections, poor orientation, extensive loss of IEL alone and attenuation of the media in the absence of fibrosis often made the consensus diagnosis difficult. The patients have mean age at diagnosis of 77 (range: 48-95), with predominance of women (81%). Common clinical manifestations included headache (74%), visual symptoms (56%), and scalp tenderness (39%). A history of polymyalgia rheumatica and giant cell arteritis was noted in 26% and 11% of patients, respectively. Thirty patients (48%) were on steroid treatment for longer than 1 month prior to the biopsy. Eleven patients (18%) did not receive steroid therapy after the biopsy, while 51 patients (82%) were treated with steroids.

Conclusions: To improve the consistency in the diagnosis of HA, we find that the most reliable histopathological parameters are: (1) neovascularization of the media; (2) interruption of IEL contiguous with medial replacement fibrosis; and (3) irregular, distinctly eccentric intimal thickening. Majority of patients with initial diagnosis of HA received steroid therapy.

314 High Risk Clinical Features Correspond to a Definitive Pathologic Diagnosis and Poor Overall Outcome in Penile Calcific Uremic Arteriolopathy (CUA)

Jason Singh[1], Viraj Master[2], Carla Ellis[2]
[1]Emory University Hospital, Atlanta, GA, [2]Emory University, Atlanta, GA

Disclosures: Jason Singh: None; Viraj Master: None; Carla Ellis: None

Background: Penile calcific uremic arteriolopathy (CUA), also known as calciphylaxis, is a rare but highly morbid complication of end stage renal disease. Biopsy of the lesion is contraindicated; however parathyroidectomy and/or penectomy can prolong survival and control pain and infection. Definitive diagnostic criteria do not exist; however, clinical features specific to CUA have been described, and may aid in differentiating lesions secondary to atherosclerosis or infection from those of CUA.

Design: A search of our pathology data system using the term "penectomy" was performed and cases with a neoplastic diagnosis were excluded. High risk **clinical** features were defined as any patient with end stage renal disease (ESRD) plusat least 3 of 4 of the following: diabetes mellitus, pain on physical exam, pelvic arterial calcifications diagnosed on imaging studies and an increased calcium phosphate product. High risk **histopathologic** features were defined as patients having at least one of either of the following: medial arterial/arteriolar calcification or arteriolar thrombosis. Age, ethnicity, history of hypertension, insulin dependence and follow up data were also obtained.

Results: 21 cases were found, of which 9/21 specifically used the term "CUA" and 12/21 used other descriptive wording in the diagnosis line. Descriptive wording included "gangrene", "necrosis" and "atherosclerotic calcifications". 19/21 (90%) patients were African-American (AA), and the mean age at surgery was 57 years. 7/21 (33%) cases were high clinical risk. 20/21 (95%) cases were high histopathologic risk. 6/7 high clinical risk patients and 3/14 non-high clinical risk patients had "CUA" in the diagnosis line (p=0.005). Whereas 6/7 high clinical risk and 14/14 non-high clinical risk patients had high risk histopathologic findings (not statistically significant). 6/7 high clinical risk patients and 4/14 non-high clinical risk patients were dead at follow up (p=0.134). Average follow up time was 21 months post-surgery.

Conclusions: Clinical findings necessitating penectomy in non-neoplastic penile disease are much more common in AA men. High risk clinical findings associated with CUA correspond to a definitive wording of the pathologic diagnosis and a poor overall outcome. Histopathologic findings are not specific, and the contraindication of a biopsy in this setting further illustrates the need for a focused clinical assessment, utilizing the clinical features described and potentially including AA ethnicity.

315 Cardiomyocyte reverse remodeling following left ventricular assist device (LVAD) implantation: a morphometric and cytogenetic analysis

Nicholas Stanzione[1], Gregory Fishbein[1], Nagesh Rao[2]
[1]David Geffen School of Medicine at UCLA, Los Angeles, CA, [2]UCLA School of Medicine, Los Angeles, CA

Disclosures: Nicholas Stanzione: None; Gregory Fishbein: None; Nagesh Rao: None

Background: Myocardial remodeling in heart failure patients is accompanied by an increase in cell size, myocyte hypertrophy, and DNA replication. Due to the inability of cardiomyocytes to divide, this leads to polyploidy and occasional multinucleation. In some cases, when supported by a left ventricular assist device (LVAD), the heart undergoes reverse remodeling and returns to normal size with improved function. The goal of this study is to evaluate whether the morphologic and cytogenetic nuclear changes of myocyte hypertrophy can be reversed following LVAD support.

Design: We performed a retrospective review of patients bridged to heart transplant with an LVAD from 2012-2018, with at least 9 months of LVAD support prior to transplantation. Six patients met the inclusion criteria. H&E sections of the apical core from the time of LVAD placement and routine sections from the explanted hearts were reviewed. We measured the average cell width and nuclear area of 20 well-oriented myocytes in areas without focal pathologic changes. Fluorescent in-situ hybridization (FISH) studies were performed using two sets of three multicolored probes for chromosomes X, Y, 18 and 3, 7, 9p, 17, with 200 nuclei analyzed per specimen.

Results: The cohort is composed of 3 males and 3 females. Their underlying diseases include: hypertrophic cardiomyopathy (HCM), ischemic heart disease, and 4 cases of dilated cardiomyopathy. The average duration of LVAD support was 19 months (10-37). Preliminary FISH studies show a high degree of polyploidy in explanted hearts despite LVAD support (Fig 1). Direct comparison of aneuploidy before and after LVAD implantation is currently pending. Morphometry showed up to 51% decrease in nuclear area after 19 months of support with an LVAD (Fig 2). An increase in nuclear area was seen in 2 cases.

Figure 1 - 315

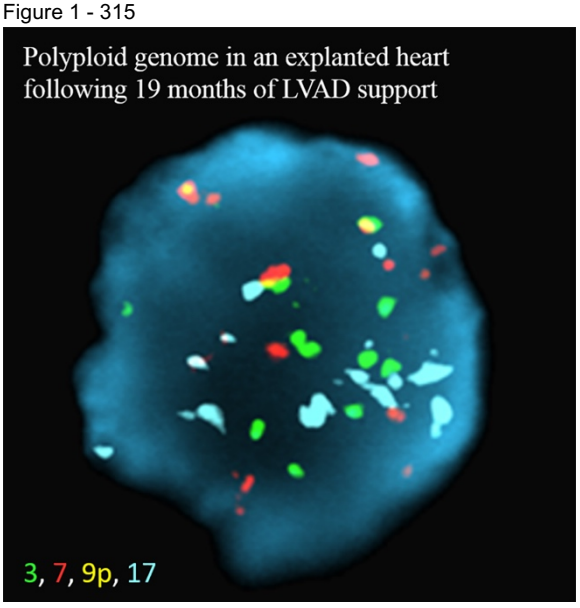

Figure 2 - 315

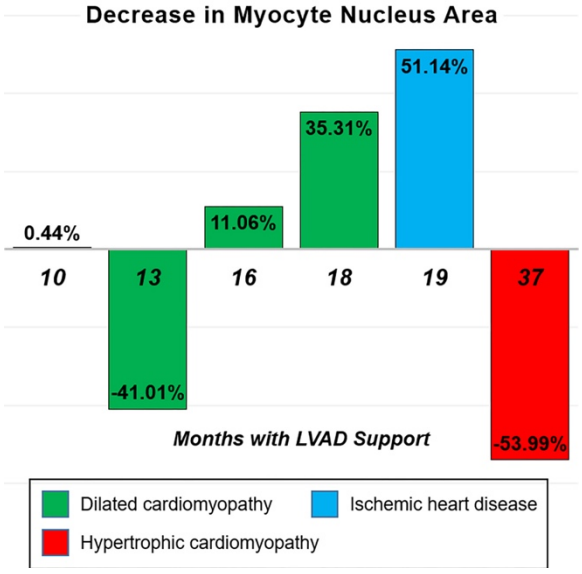

Conclusions: Four of the 6 cases demonstrated a reduction in nuclear area after LVAD support. The degree of interval decrease in these cases appeared to increase with longer duration of LVAD support. One of the cases that showed an interval increase in nuclear area was a case of HCM; we postulate that continued nuclear enlargement despite LVAD support in this case may represent the natural progression of the underlying cardiomyopathy. Our preliminary data suggest that the morphologic nuclear changes of hypertrophy may regress following prolonged LVAD support. FISH analysis to determine whether these changes are accompanied by a decrease in polyploidy is currently pending.

316 Cardiovascular Effects of Different Intensities of Exercise in a Model of Sympathetic Hyperactivity in Mice

Luciana Wilensky[1], German Gonzalez[1], Alejandro Emilio Masucci[1], Pablo Cassaglia[1], Celina Morales[1]
[1]Faculty of Medicine, Buenos Aires, Argentina

Disclosures: Luciana Wilensky: None; German Gonzalez: None; Alejandro Emilio Masucci: None; Pablo Cassaglia: None; Celina Morales: None

Background: The cardioprotective effects of exercise are known, however, it is believed that, the intensity at which it is performed plays a fundamental role in the development of the type of hypertrophy. In our study we aim the effects of different intensities of exercise training on myocardial hypertrophy, structural histological parameters and its impact on cardiac function (CF) in mice with a specific cardiac sympathetic hyperactivity by overexpression of the Gs? protein.

Design: Male Gs? protein overexpression mice were randomized in sedentary (Gs?SED), moderate exercise (Gs?ME) and intense exercise (Gs?IE) groups. Mice were subjected to exercise performed by swimming during 90 minutes once a day during 6 days/week in moderate exercise (ME) and twice a day in intense exercise (IE). After 4 weeks, CF was studied in catheterized animals followed a stimulation with isoproterenol (ISO) for analyzing the myocardial reserve. Then, myocyte cross sectional area (MCSA) with its respective hypertrophy index (left ventricular weight/length of the tibia), myocardial collagen concentration and capillary density were also quantified.

Results: Were expressed as: X±SEM (*p<0.05). IE increased left ventricular hypertrophy 24±5%, which was evidenced with significant increase in MCSA (?m^2) in Gs?IE group (527±23) respect both Gs?SED (354±19*) and Gs?ME (354±19*). IE tended to increase the collagen concentration while ME tended to increase capillary density, but both were no significant respect Gs?SED group (P=NS). CF was similar in all groups, except ME increased final diastolic pressure (FDP, mmHg) in Gs?ME (20±3) as compared with Gs?SED (8±2*) and Gs?IE (8±3*). In response to ISO, no differences were observed between the experimental groups.

Conclusions: Due to the sympathetic hyperactivity of the mouse model with Gs? overexpression, transgenic sedentary controls are required, for histological and functional comparison. Present results suggest that moderate exercise does not induce heart hypertrophy since they show conserved structural signs, corresponding to an intensity of beneficial exercise. However, intense exercise produces hypertrophy of 24% and a tendency to increase collagen, that did not achieve a significant value but suggests, that this greater exercise intensity could be not recommended. More evaluations could be made in exercise protocols of greater chronicity to clarify whether the exercise intensity of the Gs?IE group is over the positive level for the heart.